Published in final edited form as:
Brain Struct Funct. 2014 July ; 219(4): 1287–1303. doi:10.1007/s00429-013-0566-y.

Central stress-integrative circuits: Forebrain glutamatergic and GABAergic projections to the dorsomedial hypothalamus, medial preoptic area, and bed nucleus of the stria terminalis

Brent Myers[1], **C. Mark Dolgas**[1], **John Kasckow**[2], **William E. Cullinan**[3], and **James P. Herman**[1]

[1]Department of Psychiatry and Behavioral Neuroscience, University of Cincinnati, Cincinnati, OH, USA

[2]VA Pittsburgh Health Care System, Western Psychiatric Institute and Clinic, University of Pittsburgh Medical Center, Pittsburgh, PA, USA

[3]Department of Biomedical Sciences, Marquette University, Milwaukee, WI, USA

Abstract

Central regulation of hypothalamo-pituitary-adrenocortical (HPA) axis stress responses is mediated by a relatively circumscribed group of projections to the paraventricular hypothalamus (PVN). The dorsomedial hypothalamus (DMH), medial preoptic area (mPOA), and bed nucleus of the stria terminalis (BST) provide direct, predominantly inhibitory, innervation of the PVN. These PVN-projecting neurons are controlled by descending information from limbic forebrain structures, including the prefrontal cortex, amygdala, hippocampus, and septum. The neurochemical phenotype of limbic circuits targeting PVN relays has not been systematically analyzed. The current study combined retrograde tracing and immunohistochemistry/*in situ* hybridization to identify the specific sites of glutamatergic and GABAergic inputs to the DMH, mPOA, and BST. Following Flouro-Gold (FG) injections in the DMH, retrogradely-labeled cells co-localized with vesicular glutamate transporter mRNA in the prefrontal cortex, ventral hippocampus, and paraventricular thalamus. Co-localization of FG and glutamic acid decarboxylase mRNA was present throughout the central and medial amygdaloid nuclei and septal area. Additionally, the mPOA received predominantly GABAergic input from the septum, amygdala, and BST. The BST received glutamatergic projections from the hippocampus and basomedial amygdala, whereas GABAergic inputs arose from central and medial amygdaloid nuclei. Thus, discrete sets of neurons in the hypothalamus and BST are positioned to summate limbic inputs into PVN regulation and may play a role in HPA dysfunction and stress-related illness.

Keywords

Retrograde tracing; amygdala; prefrontal cortex; vesicular glutamate transporter; glutamic acid decarboxylase; hypothalamo-pituitary-adrenal axis

Address for correspondence: Brent Myers, Ph.D. University of Cincinnati Metabolic Diseases Institute 2170 E. Galbraith Rd Cincinnati OH 45237-0506 Tel: 513 558 3029 Fax: 513 558 9104 brent.myers@uc.edu.

INTRODUCTION

Glutamatergic and GABAergic neurons play important roles in stress regulation, directly exciting and inhibiting, respectively, paraventricular hypothalamic (PVN) corticotropin-releasing hormone (CRH) neurons (Cole and Sawchenko, 2002, Bartanusz et al., 2004). Tract-tracing studies indicate that inhibitory GABAergic inputs to the PVN emanate from several structures in the basal forebrain and hypothalamus, including the preoptic area (POA), dorsomedial hypothalamus (DMH), and bed nucleus of the stria terminalis (BST) (Roland and Sawchenko, 1993, Boudaba et al., 1996, Radley et al., 2009). In contrast, glutamatergic inputs to the PVN originate from other hypothalamic nuclei including the posterior hypothalamus (PH), ventromedial hypothalamus (VMH), as well as DMH (Ulrich-Lai et al., 2011). Neurons in these regions, including those that project to the PVN, show pronounced activation by stressful stimuli (Cullinan et al., 1995, Cullinan et al., 1996), consistent with a role in stress regulation.

Descending input from the limbic forebrain is thought to influence the role of the DMH, POA, and BST in stress integration (Herman et al., 2003, Ulrich-Lai and Herman, 2009). These PVN-projecting regions are implicated in a variety of processes related to stress, including autonomic function, defensive behavior, and fear responses (DiMicco et al., 1996, Hakvoort Schwerdtfeger and Menard, 2008, Duvarci et al., 2009, Motta et al., 2009, Walker et al., 2009). These functions are all regulated by forebrain circuits, involving regions such as the medial prefrontal cortex (mPFC), hippocampus, medial amygdala (MeA), central amygdala (CeA), and lateral septum (LS) (Price, 2005). Notably, none of these limbic forebrain sites send substantial projections to the PVN proper. Thus, it is highly likely that their influence on hypothalamo-pituitary-adrenocortical (HPA) axis output is communicated through intervening neurons. In line with this hypothesis, dual tracing studies indicate that terminals of neurons in the ventral subiculum (vSub), which provide a major stress-inhibitory input to the PVN, can be visualized in apposition to PVN-projecting neurons in the DMH, POA, and BST (Kohler, 1990, Cullinan et al., 1993). In addition, CeA and MeA neurons, previously shown to be HPA-excitatory (Prewitt and Herman, 1994, Dayas et al., 1999, Xu et al., 1999, Solomon et al., 2010), have terminals in apposition to PVN-projecting neurons in the BST and mPOA (Prewitt and Herman, 1998). Collectively, these studies suggest that forebrain modulation of medial parvocellular PVN neurons occurs through connections in these three intervening nuclei.

The neurochemical signature of limbic-PVN relays remains to be determined. Descending inhibitory inputs from the mPFC and hippocampus (vSub) are postulated to be glutamatergic (Ulrich-Lai and Herman, 2009, Radley and Sawchenko, 2011), presumably interacting with PVN-projecting GABA neurons in the basal forebrain and hypothalamus. In contrast, HPA excitation is believed to be mediated largely by the amygdala (Shepard et al., 2003, Myers et al., 2012). Projection neurons of this region are predominantly GABAergic, and thus predict GABA-GABA disinhibition at the level of the PVN. To evaluate these putative circuits, the current study maps GABA and glutamate neurons in limbic regions known to modulate stress activation to examine the phenotype of limbic projections to primary basal forebrain and hypothalamic PVN-projecting cell populations.

METHODS

Animals

Male Sprague-Dawley rats (250-300 g; Harlan, Indianapolis, IN) were housed individually in standard rat cages. Rats were maintained in a temperature- and humidity-controlled room (lights on 06:00 to 18:00) with food and water available *ad libitum*. All experimental procedures and protocols were conducted in accordance with the National Institutes of Health Guidelines for the Care and Use of Laboratory Animals and approved by the University of Cincinnati Institutional Animal Care and Use Committee.

Retrograde tracer injections

Animals were anesthetized with ketamine (87 mg/kg) and xylazine (13 mg/kg) and prepared for aseptic stereotaxic surgery. Briefly, the scalp was incised and burr holes drilled in the skull in accordance with the planned injection coordinates. Glass micropipettes (10-15 μm tips) filled with 4% Flouro-Gold (FG) were lowered into place and left for 10 min prior to injection. Coordinates for the injections were as follows: dorsomedial hypothalamus, 3.3 mm caudal to bregma, 0.5 mm lateral to midline, and 8.5 mm ventral from skull (n = 12); ventrolateral medial preoptic area, 0.8 mm caudal to bregma, 0.8 mm lateral to midline, and 8.4 mm ventral from skull (n = 12); and principal/intrafascicular subnulcei of the BST, 0.8 mm caudal to bregma, 1.2 mm lateral to midline, and 6.5 mm ventral from skull (n = 12). FG was transferred by iontophoresis (3 min, 5 mA, 8 sec alternating current pulses). Micropipettes were left in place for 10 min (to prevent backflow up the pipette track), at which point the burr hole was packed with sterile bonewax and the incision closed with wound clips. Animals were euthanized one week following injection by overdose with Pentobarbital (150 mg/kg) and perfused with 100-150 ml phosphate-buffered saline (PBS), followed by 250 ml of 4% paraformaldehyde. Following perfusion, brains were removed and placed in fixative solution for one hour, after which they were transferred to 30% sucrose for cryoprotection. Brains were then sectioned at 25 μm on a Microm sliding microtome and stored in DEPC-treated cyroprotectant solution (30% sucrose, 30% ethylene glycol, 1% polyvinylpyrrolidone in sodium phosphate buffer).

Flouro-Gold immunohistochemistry

FG injection sites were verified by immunohistochemistry using an anti-FG antibody, courtesy of Dr. Stanley Watson, University of Michigan. Methods for visualization of FG immunoreactivity have been previously published (Ulrich-Lai et al., 2011); briefly, a series of sections was removed from cryoprotectant, washed 5 × 5 minutes in potassium PBS (KPBS) (50 mM, pH 7.4), blocked in 4% normal rabbit serum in KPBS for 30 min and subsequently incubated in primary antiserum overnight (diluted 1:5000; in KPBS containing 1% normal rabbit serum and 0.5% Triton-X 100). On the second day, sections were rinsed in KPBS (5 × 5 minutes), incubated in biotinylated goat anti-rabbit IgG (diluted 1:500 in KPBS) for one hour, rinsed again in KPBS (5 × 5 minutes) and subsequently incubated in avidin-biotinylated peroxidase complex (ABC Elite solution, Vector labs) for one hour (diluted 1:500 in KPBS). At the conclusion of this incubation, sections were again rinsed (5 × 5 minutes) and reaction product visualized using diaminobenzidine and hydrogen peroxide.

Combined immunohistochemistry/in situ hybridization

Preparation of cRNA probes for vesicular glutamate transporter 1 (vGluT1), 2 (vGluT2), and glutamic acid decarboxylase 65 (GAD65) mRNAs was carried out as previously described (Bowers et al., 1998, Ziegler et al., 2002, Ulrich-Lai et al., 2011, Ziegler et al., 2012). Combined immunohistochemistry/*in situ* hybridization was also performed as described previously (Cullinan et al., 2008, Ulrich-Lai et al., 2011, Ziegler et al., 2012) with some modifications. Briefly, a 1-in-6 series of sections was washed with 50 mM KPBS and incubated in blocking buffer (0.3% Triton X-100 and 0.2% bovine serum albumin in KPBS). Sections were hybridized overnight (45 °C with 4.5×10^6 cpm ^{35}S labeled probe), rinsed in 2× SSC buffer, treated with RNAse A (200 μg/mL for 3 h at 37 °C), washed in decreasing concentrations of SSC (2-0.5× at room temperature), and incubated in 0.5× SSC (1 h at 45 °C) as previously described (Ulrich-Lai et al., 2011). Sections were subsequently processed for FG immunohistochemistry (see above). FG was visualized by chromagen (diaminobenzidine) reaction to provide a stable signal for detection of co-localization in emulsion-dipped sections. Sections were mounted onto Superfrost Plus slides, dehydrated through graded ethanol, and air dried. Slides were then coated with Kodak photographic emulsion NTB2 (diluted 1:1 with water), air-dried, and stored at 4 °C in a light- and humid-free environment for 5 weeks. Following development in Kodak D-19 developer and Rapid Fix solutions, emulsion-dipped sections were counterstained with 0.25% cresyl violet, dehydrated, and coverslipped using DPX mountant (Fluka, Milwaukee, WI).

Image processing

Figures were prepared using Adobe Photoshop 7.0 for Windows. Microscopic images were captured from emulsion-dipped, counterstained slides using a Zeiss Axiocam digital camera. All images were imported into Photoshop and brightness/contrast adjusted to provide optimal visualization.

Analysis

Neuroanatomical regions were identified with reference primarily to Swanson's rat brain atlas (Swanson, 2004). Positively-labeled neurons were identified as having grain densities greater than 5 times that of an equivalent area used to determine background levels of hybridization signal. Specifically, within tissue sections being analyzed, the white matter tract nearest the region of interest was observed for the approximate number of grains per unit area (30 μm^2). FG-labeled cells exhibiting at least 5 times the background level (typically > 5-10 grains/cell) were determined to exhibit co-localization. Criteria for grading the extent of GAD65, vGluT1, or vGluT2 co-localization with FG were as follows: (-), widely scattered dual-labeled cells representing a minor subset of cells in a given region (substantially less than 25%); (+), dual-labeling in 25-50% of cells within a given nucleus; (++), dual-labeling in the majority of cells within a given nucleus (generally 50-75%); (+++), most, if not all, FG-positive cells double-labeled. Dual-labeled cells were counted on sections through the MeA to verify that the subjective measures were on target; once confidence in the scoring method was assured, analysis of remaining regions was scored as above. Scoring was performed by two individuals blind to the location of the injection site.

RESULTS

Expression of glutamate and GABA was assessed in neurons projecting to putative limbic-PVN relays in the DMH (including the dorsomedial hypothalamic nucleus and dorsal area of the hypothalamus), mPOA (including the anterior hypothalamic nucleus (AHN) and medial preoptic nucleus (MPN)), and posterior BST (including the principal, transverse, and interfasicular subregions). These regions were targeted on the basis of 1) rich projections to the PVN, 2) activation by stressful stimuli, and 3) expression of GABAergic markers. As projections to these regions have been mapped previously (Weller and Smith, 1982, Simerly and Swanson, 1986, Thompson and Swanson, 1998), the current study focused on localization of vGluT1 (**Fig. 1A**) and vGluT2 mRNA, glutamatergic markers, and GAD65 mRNA (**Fig. 1B**), a GABAergic marker, in identified limbic brain regions. Criteria for determining FG-positive cells and mRNA co-localization are demonstrated in **Fig. 1C**.

Neurochemistry of projections to the DMH

A representative DMH injection site is depicted in **Fig. 1D** and the distribution of injections into this region is summarized in **Fig. 2A**. Injections were aimed at the ventrolateral region, which sends stress-activated projections to the parvocellular PVN (Cullinan et al., 2008). As noted, several injections encompassed more of the DMH than intended, and others labeled regions outside the bounds of the ventrolateral DMH. Thus, definition of the DMH was based on well-placed cases (n = 4), while other projection regions seen in larger injections were considered to reflect projections to areas outside the principal region under analysis. Therefore, all data included in tables and figures omit regions labeled by non-specific or overly large injections.

Injections of FG confined to the DMH labeled vGluT1-positive neurons in the deep layers of the infralimbic, orbital, and, to a lesser extent, prelimbic cortices (**Table 1** and **Fig. 3**). In addition, a subset of ventral subicular neurons was labeled with FG and vGluT1, as well as a small number of neurons in ventral CA1. Small aggregations of cells were also observed in the agranular insular cortices and the dorsal endopiriform cortex. No significant retrograde labeling was observed in other cortical or hippocampal regions. The vast majority of FG-labeled cells in cortical regions were GAD65 negative. This was also the case with the more limited labeling seen in the ventral hippocampal regions. Whereas GAD65 mRNA was scattered throughout all the labeled cortical regions, co-localization with FG was rare, consistent with a substantial body of literature indicating that GABA is generally contained in interneurons of the cortex and hippocampus (Somogyi et al., 1985). Additionally, the DMH received substantial vGluT2-positive input from the extreme dorsal region of the paraventricular thalamus (PVT) (**Fig. 2B**).

The intermediate and ventrolateral subdivisions of the LS and the fusiform (**Fig. 2C**) and anteroventral subnuclei of the BST showed substantial aggregations of FG-labeled, GAD65-positive neurons. Retrogradely-labeled GABAergic neurons were also observed in the medial division of CeA (**Fig. 2D**) and posteroventral and posterodorsal subnuclei of the MeA. Mixed glutamatergic and GABAergic input was received from the PH and lateral hypothalamus (LH). Inputs from the AHN and MPN were primarily GABAergic, as was the limited input from nucleus accumbens (NAc). Additional GAD65-positive projections

included the sub-PVN zone, peri-PVN, peri-supraoptic nucleus region, and ventromedial zona incerta. Input from the periaqueductal gray (PAG) emanated primarily from the rostral and dorsolateral regions and was generally seen in cases that involved the dorsolateral DMH.

Neurochemistry of projections to the mPOA

Injections were targeted to the ventrolateral region of the medial preoptic area (corresponding to the ventral AHN). Previous reports demonstrate robust c-Fos induction in this region by numerous stressors (Cullinan et al., 1995) and it sends GABAergic projections to the parvocellular PVN (Boudaba et al., 1996, Cullinan et al., 2008). The distribution of injections (n = 5) is summarized in **Fig. 4A**. As noted, several cases with AHN injections spread to MPN, which also projects to the PVN (Cullinan et al., 1996).

Injections limited to the AHN produced FG labeling in numerous stress-regulatory limbic areas, most notably in the MeA, rostral and intermediate zones of the LS, and perifornical and posterior hypothalamic regions (LH and PH). Prefrontal cortical neurons displayed sparse FG labeling; however, injections into the more rostrally-situated MPN resulted in substantial FG labeling in the vSub/ventral CA1 region. Hippocampal input to the AHN and MPN was glutamatergic (vGluT1 mRNA positive), as was the case for input from the PVT (vGluT2 mRNA positive) (**Table 2** and **Fig. 5**).

The AHN received rich GABAergic innervation from the LS (**Fig. 4B**), ventrolateral BST (**Fig. 4C**), and posterodorsal MeA (**Fig. 4D**). Injections spreading to the MPN extensively labeled neurons throughout the BST, most heavily in the principal nucleus, as well as anteroventral and posteroventral subdivisions of the MeA and medial division of the CeA. Input from the BST and amygdala was virtually all GABAergic. In addition, small numbers of retrograde labeled-GAD65 mRNA positive neurons were observed in the NAc shell.

Numerous hypothalamic regions sent mixed glutamatergic and GABAergic projections to the AHN. Included among these are the ventrolateral and dorsolateral DMH and perifornical LH, where greater than half of the observed FG immunoreactive neurons were GABAergic. In contrast, co-localization of GAD65 and FG was seen in substantially less than half of the projection neurons from the PH and projections from the VMH and mammillary nuclei were largely vGluT2 positive. The AHN received input from the medial and ventrolateral divisions of the PAG, a minority of which were GABAergic. This pattern contrasts with that of injections involving the MPN, which received a sizable yet similarly mixed GABAergic innervation from the extreme rostromedial region.

Neurochemistry of projections to BST subregions

FG injections were targeted to posterior BST subnuclei (**Fig. 6A**) (principal, transverse, and interfasicular), representing a BST region that 1) is implicated in modulation of HPA axis tone (Choi et al., 2007) and 2) contains large numbers of PVN-projecting neurons (Boudaba et al., 1996). Due to the complex and irregular organization of the BST, FG injections typically encompassed more than one discrete subdivision with some of the more rostral injections hitting the anterodorsal and anteromedial subnuclei. Therefore, only cases limited

to the posterior BST subnuclei (n = 3) are included in **Figures 6-7** and **Table 3**; however, several cases confined to the anterior subnuclei of the BST are discussed in terms of anterior-posterior afferent heterogeneity.

In all cases, FG-labeled neurons were richly localized to the posterodorsal MeA and basomedial amygdala (BMA). Posterior BST injections revealed numerous glutamatergic projection neurons in ventral CA1 (**Table 3** and **Fig. 7**), vSub (**Fig. 6B**), anterior and posterior cortical amygdaloid nuclei (CoA), posterior amygdala, and, to a lesser extent, the basolateral subnuclei of the amygdala. In fact, the number of retrograde-labeled, glutamate-positive neurons in the hippocampus and amygdala greatly outnumbered that seen following either DMH or mPOA injections. In contrast, the number of retrogradely-labeled neurons in the mPFC was much sparser. Additionally, numerous FG-positive neurons were observed in the anterior PVT (**Fig. 6C**), medial subdivision of the nucleus reunions, and posterior intralaminar nucleus. In all cases, thalamic projections were predominantly vGluT2 mRNA positive.

The vast majority of FG-containing neurons in the posterodorsal and anterodorsal MeA were GAD65 mRNA positive. Unlike the posterodorsal and anterodorsal projections of the MeA, BST inputs from the posteroventral MeA included both GABAergic and glutamatergic cells. All FG-labeled neurons in the medial division of the CeA were GABAergic (**Fig. 6D**) with some co-localization also in the lateral CeA. The BST received GABAergic inputs from other basal forebrain regions including a predominantly (but not exclusively) GABAergic input from the dorsal LS. Strong GABAergic inputs to both anterior and posterior BST regions were also observed in the NAc shell, ventral limb of the diagonal band of Broca, substantia innominata, and subthalamic zona incerta.

The hypothalamus provided rich GABAergic innervation to all levels of the BST. Perhaps the densest GABAergic hypothalamic projection to the BST emanated from the MPN. Large numbers of GAD65-positive, FG-labeled cells were also observed in the AHN, sub-PVN zone, and peri-PVN region. Mixed populations of glutamatergic and GABAergic cells were observed in the LH and the ventrolateral and dorsolateral DMH. Largely vGluT2-positive BST projections were observed originating in the PH, VMH, medial mammillary nucleus, and supramammillary nucleus. In general, midbrain projections to the BST were less pronounced than those of the DMH or mPOA (some FG neurons were evident in the commissural subnucleus of the PAG).

Although there was substantial overlap of inputs to the anterior and posterior subnuclei of the BST, there were some notable differences. Specifically, posteriorly-placed injections typically labeled more of ventral CA1 and vSub than did injections involving anterodorsal components of the BST. There was also a rostro-caudal gradient in the strength of innervation from the MeA as the number of double-labeled neurons in the MeA was greatest following injections into posterior divisions of the BST. In contrast, GABAergic innervation from the dorsal LS was more pronounced following anterior BST injections. There were also substantial differences in the weight of hypothalamic inputs to the anterior and posterior BST subnuclei. Labeling in the ventrolateral and dorsolateral DMH, AHN, sub-PVN zone,

and peri-PVN region was more prominent following posterior BST injections, while LH and VMH projections favored the anterior BST.

Methodological Considerations

The current studies employed an approach requiring simultaneous localization of both mRNA and protein, using sequential techniques. Thus, it is possible that the combination of techniques may have resulted in the loss of protein and/or *in situ* hybridization signal. The results are generally consistent with previous FG tracing studies and both the vGluT and GAD *in situ* hybridizations yielded robust and intense cellular signals. However, it remains possible that the combination of techniques underestimated the number of vGluT and GAD mRNA positive, FG-labeled neurons. In addition, the nature of the combined approach yields grains in an emulsion layer that overlies the immunoreactivity within the tissue section. Thus, the separation of the signals in space as well as issues related to probe penetration and emission may have limited the ability to definitively co-localize signal, and resulted in an underestimate of the number of dual-labeled neurons. Another consideration relates to the labeling of inputs to surrounding structures based on small differences in injection placement and/or the iontophoretic procedure itself affecting tracer uptake at the core of the injection site. Consequently, these methodological limitations led us to temper our conclusions and we endeavored to make conservative estimates of co-localization to minimize false positive identifications.

DISCUSSION

Our results demonstrate a pronounced, chemically-specific, limbic forebrain innervation of PVN-projecting regions of the DMH, mPOA, and BST. Innervation of the predominantly GABAergic DMH, mPOA, and BST by GABAergic neurons of the MeA and CeA supports the hypothesis that these amygdalar regions promote HPA axis activation by disinhibition, using sequential GABAergic synapses. Moreover, the data also indicate a prominent GABAergic innervation from LS subnuclei, suggesting that this area may participate in stress excitation as well. In contrast, there is evidence for excitatory innervation of the DMH, mPOA, and BST by hippocampal and prefrontal cortical neurons, consistent with the glutamatergic signature of outputs from these stress-inhibitory sites. Finally, and importantly, all three PVN-projecting regions receive mixed GABA and glutamate input from hypothalamic nuclei which may be relevant to intra-hypothalamic mechanisms governing the integration of stress responses.

Implications for DMH stress circuits: homeostatic integration

The DMH is extremely important for integrating hormonal, cardiovascular, and behavioral stress responses (Shekhar, 1993, Bailey and Dimicco, 2001, Kerman et al., 2006, Fontes et al., 2011). As an upstream regulator of the PVN, the DMH is highly sensitive to psychogenic stressors (Cullinan et al., 1995). With regard to HPA axis integration, the ventrolateral subdivision of the DMH sends stress-activated GABAergic projections to the PVN (Cullinan et al., 2008). The vast majority of these PVN-projecting neurons contain GAD65, indicating that this is likely a stress-inhibitory region of the DMH. In contrast, the dorsomedial portion of the DMH predominantly expresses vGluT2 and provides

glutamatergic innervation of the PVN (Ulrich-Lai et al., 2011). Our group has demonstrated that local injection of a panionotropic glutamate receptor antagonist into the DMH enhances corticosteroid responses to restraint stress (Ziegler and Herman, 2000, Herman et al., 2003), consistent with removal of glutamate drive to this region. Microstimulation of the dorsal component of the DMH results in an increase in ACTH release while inhibition has the opposite effect (Bailey and Dimicco, 2001, Morin et al., 2001). However, the dorsal portion of the DMH does not contain large quantities of Fos-activated neurons following stress (Cullinan et al., 1995, Cullinan et al., 2008). Therefore, it is possible that this area is involved in other homeostatic processes.

The current study revealed that the LS is a primary site of GABAergic input to the DMH (**Fig. 8**). The DMH projection from the septum emanated from both the intermediate region and the ventrolateral region, an area that shows extensive Fos activation following psychogenic stress (Cullinan et al., 1995). The chemistry of this pathway predicts an excitatory influence of the LS on the HPA axis, although this prediction does not agree with previous studies documenting a stress-excitatory effect of LS lesions on the HPA axis (Singewald et al., 2011) or the well-documented “septal rage” symptoms that occur after LS lesions (Gotsick and Marshall, 1972, Schnurr, 1972). Thus, the overall functional connectivity of the LS may be more complicated and warrants further investigation. The DMH also received GABAergic input from neurons of the ventrolateral and fusiform subnuclei of the anterior BST. This region of the BST has been implicated in HPA axis and autonomic excitation (Dong et al., 2001b). Thus, the DMH may serve as conduit for stress activation of neurosecretory and pre-autonomic neurons. The DMH was also targeted by GABAergic and glutamatergic inputs from numerous hypothalamic nuclei, including the LH and PH. The LH is essential for integrating metabolic and motivational signals (Davis et al., 2011), and projections to the DMH may be a component of LH visceromotor output. Furthermore, the PH is a key site for cardiovascular regulation (DiMicco et al., 1986, Lisa et al., 1989) and projections to the DMH may constitute another means for the integration of homeostatic and limbic circuits.

Implications for mPOA stress circuits: androgenic influence

Previous studies indicate the importance of the mPOA, encompassing the MPN and AHN, in inhibition of HPA function (Viau and Meaney, 1996). Viau and colleagues demonstrated that lesions of the mPOA increase stress-induced ACTH and corticosterone release while stimulation of the area decreases HPA activation (Viau and Meaney, 1996, Williamson and Viau, 2008). Importantly, the mPOA mediates the inhibitory effects of testosterone on the HPA axis, likely associated with large numbers of androgen and estrogen receptor-expressing neurons in the MPN (Williamson and Viau, 2007, Williamson et al., 2010). Neurons in the mPOA, particularly the AHN, are Fos-activated following exposure to multiple stressors (Cullinan et al., 1995). Indeed, the AHN contains large numbers of PVN-projecting, Fos-activated neurons; the vast majority of which are GABAergic (Roland and Sawchenko, 1993, Boudaba et al., 1996, Cullinan et al., 1996), suggesting that this area mediates inhibition of the PVN.

Our results demonstrate that the densest GABAergic projections to the mPOA come from the rostral LS (**Fig. 9**). The mPOA also received inhibitory input from the posterodorsal MeA and injections centered on the MPN labeled predominantly GABAergic neurons in the anterodorsal MeA. Small numbers of retrogradely-labeled GABAergic neurons were present in nearly all BST subnuclei and the NAc shell, suggesting the mPOA may play a role in disinhibition of the HPA axis by these regions. Like the DMH, the mPOA was richly innervated by mixed neurotransmitter input from numerous hypothalamic nuclei, most heavily by the LH, PH, and ventrolateral DMH. Additionally, major glutamatergic projections from the VMH may play a role in regulating the impact of the mPOA on HPA axis function. Thus, like the DMH, the mPOA receives input from both glutamatergic and GABAergic limbic sites and may summate the influence of these structures on autonomic and neuroendocrine neurons in the PVN.

Implications for BST stress circuits: anterior and posterior differentiation

Previous work from our group indicates that lesions of the posterior BST increase CRH expression in the PVN as well as ACTH and corticosterone release following stress (Choi et al., 2007, Choi et al., 2008b), consistent with an inhibitory influence on HPA axis function. Anterior regions of the BST appear to have opposite effects on HPA axis regulation. Lesions of the BST encompassing most of the anterior subnuclei reduce CRH mRNA expression in the PVN and stress-induced ACTH and corticosterone secretion (Choi et al., 2007, Choi et al., 2008a), consistent with an excitatory drive to the HPA axis. In contrast with the posterior BST, anterior BST subnuclei send limited direct projections to the medial parvocellular PVN, mainly via the anteromedial and fusiform subdivisions (Dong et al., 2001b, Dong and Swanson, 2004, 2006a). Thus, it is possible that HPA axis excitation by the anterior BST may be indirect, occurring via intervening structures. In addition, the fusiform nucleus contains neurons that express CRH (Swanson et al., 1983), which is HPA axis-excitatory (Rivier and Vale, 1985).

Another important consideration for understanding BST interactions with the PVN is the relative innervation of autonomic regions of the PVN. Whereas the posterior subnuclei heavily innervate the CRH-containing region of the PVN, anterior BST regions project extensively to autonomic subdivisions (Dong et al., 2001b, Dong and Swanson, 2006a, 2006b). Thus, the anterior BST is well-positioned to affect cardiovascular responses to stressful stimuli via pre-autonomic PVN neurons. It is of interest to note that the CeA, which disproportionately innervates anterior and ventrolateral components of the BST (Dong et al., 2001a, Bienkowski and Rinaman, 2012), is implicated in the generation of autonomic responses to stress (LeDoux et al., 1988). While the CeA is thought to direct these functions largely through the brainstem (nucleus of the solitary tract, lateral parabrachial nucleus), it is possible that disinhibition of the pre-autonomic PVN by BST neurons may be an additional pathway mediating amygdala-driven autonomic stress responses.

Our data confirmed that the BST is a major target of GABAergic input from the MeA and CeA (Dong et al., 2001a). The BST received by far the greatest amount of limbic input of any of the regions studied. In addition to projections from MeA and CeA, the BST received massive input from the vSub, ventral CA1, posterior CoA, and PVT (**Fig. 10**). Substantial

input was also received from the BLA, BMA, and medial nucleus reunions. Importantly, retrogradely-labeled neurons in all of these regions were predominantly glutamatergic. The fact that this region received diverse projections from glutamatergic limbic nuclei supports the hypothesis that the posterior BST relays inhibition to the PVN.

Comparison of anterior and posterior BST FG injections revealed different patterns of input from the amygdala. Anterodorsal injections typically labeled proportionally more neurons in the medial subnucleus of the CeA (GABAergic) and BLA nuclei (glutamatergic), whereas inputs from the largely GABAergic posterodorsal division of the MeA were less pronounced. Notably, this pattern was reversed in posterior BST injections. Overall, the rich GABAergic innervation of all BST regions by amygdalar subnuclei suggests that the amygdala has the capacity to confer both inhibition and disinhibition to the PVN.

Given that all regions of the BST received both excitatory (glutamate) and inhibitory (GABA) projections from limbic forebrain and thalamic structures, it is probable that this region performs some degree of summation of these inputs, resulting in signals directed at both neuroendocrine and pre-autonomic divisions of the PVN. The subregional differences in the impact of lesions on HPA physiology are likely related to either the relative weighting of excitatory and inhibitory inputs to BST output neurons, or to the topography of inputs to these areas.

Agreement with previous studies and future directions

Our study employed the retrograde tracer FG injected into PVN-projecting areas of the BST and hypothalamus, producing similar results to previous reports utilizing anterograde tracers in the limbic forebrain. For instance, anterograde tracer injections in the vSub led to terminal labeling in the DMH, POA, and BST (Kohler, 1990, Cullinan et al., 1993). In addition, multiple reports of anterograde tracing from subnuclei of the amygdala describe terminals throughout the DMH, POA, and BST (Canteras et al., 1992, 1995, Prewitt and Herman, 1998, Dong et al., 2001a). The BST and hypothalamus have also been described as targets of the LS (Staiger and Nurnberger, 1991), NAc (Conrad and Pfaff, 1976, Groenewegen and Russchen, 1984), and PVT (Vertes and Hoover, 2008). However, a discrepancy between the present study and previous anterograde experiments relates to innervation from the mPFC. Although we discovered robust prefrontal input to the DMH, innervation of the BST was very sparse. Several reports suggest that PFC efferents target the BST (Hurley et al., 1991, Vertes, 2004, Radley et al., 2009), yet we were unable to replicate these findings. This difference may relate to the more caudal targeting of our BST injections as previous work suggests the mPFC may preferentially target the more rostral subnuclei of the BST.

Collectively, the current study suggests that there is not a single pathway for mediating stress inhibition or excitation. Instead, a highly integrated network of chemically and anatomically diverse sites coordinates the overall needs of the organism with appropriate physiological and behavioral responses to homeostatic challenge. The present results also point to the importance of tightly-regulated activity within these homeostatic circuits for maintaining appropriate stress responding and avoiding stress-related illness. Consequently, future, circuit-based approaches to the structure and function of limbic networks may help identify the aberrant circuitry responsible for stress-associated pathologies.

Acknowledgments

This work was supported by NIH grants MH049698, MH069725, MH069860, and MH090574 to JPH. The authors wish to thank Chun Xiao and Dana Ziegler for technical assistance.

ABBREVIATIONS

AHN	anterior hypothalamic nucleus
BMA	basomedial amygdala
BST	bed nucleus of the stria terminalis
CeA	central nucleus of the amygdala
CoA	cortical amygdala
CRH	corticotrophin-releasing hormone
DMH	dorsomedial hypothalamus
FG	flouro-gold
GAD65	glutamic acid decarboxylase 65
HPA	hypothalamo-pituitary-adrenal
LH	lateral hypothalamus
LS	lateral septum
MeA	medial nucleus of the amygdala
mPFC	medial prefrontal cortex
MPN	medial preoptic nucleus
NAc	nucleus accumbens
PAG	periaqueductal gray
PH	posterior hypothalamus
POA	preoptic area
PVN	paraventricular nucleus of the hypothalamus
PVT	paraventricular nucleus of the thalamus
vGluT1	vesicular glutamate transporter 1
vGluT2	vesicular glutamate transporter 2
VMH	ventromedial hypothalamus
vSub	ventral subiculum

REFERENCES

Bailey TW, Dimicco JA. Chemical stimulation of the dorsomedial hypothalamus elevates plasma ACTH in conscious rats. Am J Physiol Regul Integr Comp Physiol. 2001; 280:R8–15. [PubMed: 11124128]

Bartanusz V, Muller D, Gaillard RC, Streit P, Vutskits L, Kiss JZ. Local gamma-aminobutyric acid and glutamate circuit control of hypophyseotrophic corticotropin-releasing factor neuron activity in the paraventricular nucleus of the hypothalamus. Eur J Neurosci. 2004; 19:777–782. [PubMed: 14984429]

Bienkowski MS, Rinaman L. Common and distinct neural inputs to the medial central nucleus of the amygdala and anterior ventrolateral bed nucleus of stria terminalis in rats. Brain Struct Funct. 2012

Boudaba C, Szabo K, Tasker JG. Physiological mapping of local inhibitory inputs to the hypothalamic paraventricular nucleus. J Neurosci. 1996; 16:7151–7160. [PubMed: 8929424]

Bowers G, Cullinan WE, Herman JP. Region-specific regulation of glutamic acid decarboxylase (GAD) mRNA expression in central stress circuits. J Neurosci. 1998; 18:5938–5947. [PubMed: 9671680]

Canteras NS, Simerly RB, Swanson LW. Connections of the posterior nucleus of the amygdala. J Comp Neurol. 1992; 324:143–179. [PubMed: 1430327]

Canteras NS, Simerly RB, Swanson LW. Organization of projections from the medial nucleus of the amygdala: a PHAL study in the rat. J Comp Neurol. 1995; 360:213–245. [PubMed: 8522644]

Choi DC, Evanson NK, Furay AR, Ulrich-Lai YM, Ostrander MM, Herman JP. The anteroventral bed nucleus of the stria terminalis differentially regulates hypothalamic-pituitary-adrenocortical axis responses to acute and chronic stress. Endocrinology. 2008a; 149:818–826. [PubMed: 18039788]

Choi DC, Furay AR, Evanson NK, Ostrander MM, Ulrich-Lai YM, Herman JP. Bed nucleus of the stria terminalis subregions differentially regulate hypothalamic-pituitary-adrenal axis activity: implications for the integration of limbic inputs. J Neurosci. 2007; 27:2025–2034. [PubMed: 17314298]

Choi DC, Furay AR, Evanson NK, Ulrich-Lai YM, Nguyen MM, Ostrander MM, Herman JP. The role of the posterior medial bed nucleus of the stria terminalis in modulating hypothalamic-pituitary-adrenocortical axis responsiveness to acute and chronic stress. Psychoneuroendocrinology. 2008b; 33:659–669. [PubMed: 18378095]

Cole RL, Sawchenko PE. Neurotransmitter regulation of cellular activation and neuropeptide gene expression in the paraventricular nucleus of the hypothalamus. J Neurosci. 2002; 22:959–969. [PubMed: 11826124]

Conrad LC, Pfaff DW. Autoradiographic tracing of nucleus accumbens efferents in the rat. Brain Res. 1976; 113:589–596. [PubMed: 953754]

Cullinan WE, Helmreich DL, Watson SJ. Fos expression in forebrain afferents to the hypothalamic paraventricular nucleus following swim stress. J Comp Neurol. 1996; 368:88–99. [PubMed: 8725295]

Cullinan WE, Herman JP, Battaglia DF, Akil H, Watson SJ. Pattern and time course of immediate early gene expression in rat brain following acute stress. Neuroscience. 1995; 64:477–505. [PubMed: 7700534]

Cullinan WE, Herman JP, Watson SJ. Ventral subicular interaction with the hypothalamic paraventricular nucleus: evidence for a relay in the bed nucleus of the stria terminalis. J Comp Neurol. 1993; 332:1–20. [PubMed: 7685778]

Cullinan WE, Ziegler DR, Herman JP. Functional role of local GABAergic influences on the HPA axis. Brain Struct Funct. 2008; 213:63–72. [PubMed: 18696110]

Davis JF, Choi DL, Schurdak JD, Fitzgerald MF, Clegg DJ, Lipton JW, Figlewicz DP, Benoit SC. Leptin regulates energy balance and motivation through action at distinct neural circuits. Biol Psychiatry. 2011; 69:668–674. [PubMed: 21035790]

Dayas CV, Buller KM, Day TA. Neuroendocrine responses to an emotional stressor: evidence for involvement of the medial but not the central amygdala. Eur J Neurosci. 1999; 11:2312–2322. [PubMed: 10383620]

DiMicco JA, Abshire VM, Hankins KD, Sample RH, Wible JH Jr. Microinjection of GABA antagonists into posterior hypothalamus elevates heart rate in anesthetized rats. Neuropharmacology. 1986; 25:1063–1066. [PubMed: 3774128]

DiMicco JA, Stotz-Potter EH, Monroe AJ, Morin SM. Role of the dorsomedial hypothalamus in the cardiovascular response to stress. Clin Exp Pharmacol Physiol. 1996; 23:171–176. [PubMed: 8819648]

Dong HW, Petrovich GD, Swanson LW. Topography of projections from amygdala to bed nuclei of the stria terminalis. Brain Res Brain Res Rev. 2001a; 38:192–246. [PubMed: 11750933]

Dong HW, Petrovich GD, Watts AG, Swanson LW. Basic organization of projections from the oval and fusiform nuclei of the bed nuclei of the stria terminalis in adult rat brain. J Comp Neurol. 2001b; 436:430–455. [PubMed: 11447588]

Dong HW, Swanson LW. Projections from bed nuclei of the stria terminalis, posterior division: implications for cerebral hemisphere regulation of defensive and reproductive behaviors. J Comp Neurol. 2004; 471:396–433. [PubMed: 15022261]

Dong HW, Swanson LW. Projections from bed nuclei of the stria terminalis, anteromedial area: cerebral hemisphere integration of neuroendocrine, autonomic, and behavioral aspects of energy balance. J Comp Neurol. 2006a; 494:142–178. [PubMed: 16304685]

Dong HW, Swanson LW. Projections from bed nuclei of the stria terminalis, dorsomedial nucleus: implications for cerebral hemisphere integration of neuroendocrine, autonomic, and drinking responses. J Comp Neurol. 2006b; 494:75–107. [PubMed: 16304681]

Duvarci S, Bauer EP, Pare D. The bed nucleus of the stria terminalis mediates inter-individual variations in anxiety and fear. J Neurosci. 2009; 29:10357–10361. [PubMed: 19692610]

Fontes MA, Xavier CH, de Menezes RC, Dimicco JA. The dorsomedial hypothalamus and the central pathways involved in the cardiovascular response to emotional stress. Neuroscience. 2011; 184:64–74. [PubMed: 21435377]

Gotsick JE, Marshall RC. Time course of the septal rage syndrome. Physiol Behav. 1972; 9:685–687. [PubMed: 4670865]

Groenewegen HJ, Russchen FT. Organization of the efferent projections of the nucleus accumbens to pallidal, hypothalamic, and mesencephalic structures: a tracing and immunohistochemical study in the cat. J Comp Neurol. 1984; 223:347–367. [PubMed: 6323552]

Hakvoort Schwerdtfeger RM, Menard JL. The lateral hypothalamus and anterior hypothalamic nucleus differentially contribute to rats' defensive responses in the elevated plus-maze and shock-probe burying tests. Physiol Behav. 2008; 93:697–705. [PubMed: 18164736]

Herman JP, Figueiredo H, Mueller NK, Ulrich-Lai Y, Ostrander MM, Choi DC, Cullinan WE. Central mechanisms of stress integration: hierarchical circuitry controlling hypothalamo-pituitary-adrenocortical responsiveness. Front Neuroendocrinol. 2003; 24:151–180. [PubMed: 14596810]

Hurley KM, Herbert H, Moga MM, Saper CB. Efferent projections of the infralimbic cortex of the rat. J Comp Neurol. 1991; 308:249–276. [PubMed: 1716270]

Kerman IA, Akil H, Watson SJ. Rostral elements of sympatho-motor circuitry: a virally mediated transsynaptic tracing study. J Neurosci. 2006; 26:3423–3433. [PubMed: 16571749]

Kohler C. Subicular projections to the hypothalamus and brainstem: some novel aspects revealed in the rat by the anterograde Phaseolus vulgaris leukoagglutinin (PHA-L) tracing method. Prog Brain Res. 1990; 83:59–69. [PubMed: 2392571]

LeDoux JE, Iwata J, Cicchetti P, Reis DJ. Different projections of the central amygdaloid nucleus mediate autonomic and behavioral correlates of conditioned fear. J Neurosci. 1988; 8:2517–2529. [PubMed: 2854842]

Lisa M, Marmo E, Wible JH Jr. DiMicco JA. Injection of muscimol into posterior hypothalamus blocks stress-induced tachycardia. Am J Physiol. 1989; 257:R246–251. [PubMed: 2750964]

Morin SM, Stotz-Potter EH, DiMicco JA. Injection of muscimol in dorsomedial hypothalamus and stress-induced Fos expression in paraventricular nucleus. Am J Physiol Regul Integr Comp Physiol. 2001; 280:R1276–1284. [PubMed: 11294744]

Motta SC, Goto M, Gouveia FV, Baldo MV, Canteras NS, Swanson LW. Dissecting the brain's fear system reveals the hypothalamus is critical for responding in subordinate conspecific intruders. Proc Natl Acad Sci U S A. 2009; 106:4870–4875. [PubMed: 19273843]

Myers B, McKlveen JM, Herman JP. Neural regulation of the stress response: The many faces of feedback. Cell Mol Neurobiol. 2012; 32:683–694.

Prewitt CM, Herman JP. Lesion of the central nucleus of the amygdala decreases basal CRH mRNA expression and stress-induced ACTH release. Ann N Y Acad Sci. 1994; 746:438–440. [PubMed: 7825910]

Prewitt CM, Herman JP. Anatomical interactions between the central amygdaloid nucleus and the hypothalamic paraventricular nucleus of the rat: a dual tract-tracing analysis. J Chem Neuroanat. 1998; 15:173–185. [PubMed: 9797074]

Price JL. Free will versus survival: brain systems that underlie intrinsic constraints on behavior. J Comp Neurol. 2005; 493:132–139. [PubMed: 16255003]

Radley JJ, Gosselink KL, Sawchenko PE. A discrete GABAergic relay mediates medial prefrontal cortical inhibition of the neuroendocrine stress response. J Neurosci. 2009; 29:7330–7340. [PubMed: 19494154]

Radley JJ, Sawchenko PE. A common substrate for prefrontal and hippocampal inhibition of the neuroendocrine stress response. J Neurosci. 2011; 31:9683–9695. [PubMed: 21715634]

Rivier C, Vale W. Effect of the long-term administration of corticotropin-releasing factor on the pituitary-adrenal and pituitary-gonadal axis in the male rat. J Clin Invest. 1985; 75:689–694. [PubMed: 2982917]

Roland BL, Sawchenko PE. Local origins of some GABAergic projections to the paraventricular and supraoptic nuclei of the hypothalamus in the rat. J Comp Neurol. 1993; 332:123–143. [PubMed: 7685780]

Schnurr R. Localization of the septal rage syndrome in Long-Evans rats. J Comp Physiol Psychol. 1972; 81:291–296. [PubMed: 4563588]

Shekhar A. GABA receptors in the region of the dorsomedial hypothalamus of rats regulate anxiety in the elevated plus-maze test. I. Behavioral measures. Brain Res. 1993; 627:9–16. [PubMed: 8293308]

Shepard JD, Barron KW, Myers DA. Stereotaxic localization of corticosterone to the amygdala enhances hypothalamo-pituitary-adrenal responses to behavioral stress. Brain Res. 2003; 963:203–213. [PubMed: 12560126]

Simerly RB, Swanson LW. The organization of neural inputs to the medial preoptic nucleus of the rat. J Comp Neurol. 1986; 246:312–342. [PubMed: 3517086]

Singewald GM, Rjabokon A, Singewald N, Ebner K. The modulatory role of the lateral septum on neuroendocrine and behavioral stress responses. Neuropsychopharmacology. 2011; 36:793–804. [PubMed: 21160468]

Solomon MB, Jones K, Packard BA, Herman JP. The medial amygdala modulates body weight but not neuroendocrine responses to chronic stress. J Neuroendocrinol. 2010; 22:13–23. [PubMed: 19912476]

Somogyi P, Freund TF, Hodgson AJ, Somogyi J, Beroukas D, Chubb IW. Identified axo axonic cells are immunoreactive for GABA in the hippocampus and visual cortex of the cat. Brain Res. 1985; 332:143–149. [PubMed: 3995258]

Staiger JF, Nurnberger F. The efferent connections of the lateral septal nucleus in the guinea pig: intrinsic connectivity of the septum and projections to other telencephalic areas. Cell Tissue Res. 1991; 264:415–426. [PubMed: 1868518]

Swanson, LW. Brain Maps: Structure of the Rat Brain (3rd edition). 2004.

Swanson LW, Sawchenko PE, Rivier J, Vale WW. Organization of ovine corticotropin-releasing factor immunoreactive cells and fibers in the rat brain: an immunohistochemical study. Neuroendocrinology. 1983; 36:165–186. [PubMed: 6601247]

Thompson RH, Swanson LW. Organization of inputs to the dorsomedial nucleus of the hypothalamus: a reexamination with Fluorogold and PHAL in the rat. Brain Res Brain Res Rev. 1998; 27:89–118. [PubMed: 9622601]

Ulrich-Lai YM, Herman JP. Neural regulation of endocrine and autonomic stress responses. Nat Rev Neurosci. 2009; 10:397–409. [PubMed: 19469025]

Ulrich-Lai YM, Jones KR, Ziegler DR, Cullinan WE, Herman JP. Forebrain origins of glutamatergic innervation to the rat paraventricular nucleus of the hypothalamus: differential inputs to the anterior versus posterior subregions. J Comp Neurol. 2011; 519:1301–1319. [PubMed: 21452198]

Vertes RP. Differential projections of the infralimbic and prelimbic cortex in the rat. Synapse. 2004; 51:32–58. [PubMed: 14579424]

Vertes RP, Hoover WB. Projections of the paraventricular and paratenial nuclei of the dorsal midline thalamus in the rat. J Comp Neurol. 2008; 508:212–237. [PubMed: 18311787]

Viau V, Meaney MJ. The inhibitory effect of testosterone on hypothalamic-pituitary-adrenal responses to stress is mediated by the medial preoptic area. J Neurosci. 1996; 16:1866–1876. [PubMed: 8774455]

Walker DL, Miles LA, Davis M. Selective participation of the bed nucleus of the stria terminalis and CRF in sustained anxiety-like versus phasic fear-like responses. Prog Neuropsychopharmacol Biol Psychiatry. 2009; 33:1291–1308. [PubMed: 19595731]

Weller KL, Smith DA. Afferent connections to the bed nucleus of the stria terminalis. Brain Res. 1982; 232:255–270. [PubMed: 7188024]

Williamson M, Bingham B, Gray M, Innala L, Viau V. The medial preoptic nucleus integrates the central influences of testosterone on the paraventricular nucleus of the hypothalamus and its extended circuitries. J Neurosci. 2010; 30:11762–11770. [PubMed: 20810896]

Williamson M, Viau V. Androgen receptor expressing neurons that project to the paraventricular nucleus of the hypothalamus in the male rat. J Comp Neurol. 2007; 503:717–740. [PubMed: 17570493]

Williamson M, Viau V. Selective contributions of the medial preoptic nucleus to testosterone-dependant regulation of the paraventricular nucleus of the hypothalamus and the HPA axis. Am J Physiol Regul Integr Comp Physiol. 2008; 295:R1020–1030. [PubMed: 18685071]

Xu Y, Day TA, Buller KM. The central amygdala modulates hypothalamic-pituitary-adrenal axis responses to systemic interleukin-1beta administration. Neuroscience. 1999; 94:175–183. [PubMed: 10613507]

Ziegler DR, Cullinan WE, Herman JP. Distribution of vesicular glutamate transporter mRNA in rat hypothalamus. J Comp Neurol. 2002; 448:217–229. [PubMed: 12115705]

Ziegler DR, Edwards MR, Ulrich-Lai YM, Herman JP, Cullinan WE. Brainstem origins of glutamatergic innervation of the rat hypothalamic paraventricular nucleus. J Comp Neurol. 2012; 520:2369–2394. [PubMed: 22247025]

Ziegler DR, Herman JP. Local integration of glutamate signaling in the hypothalamic paraventricular region: regulation of glucocorticoid stress responses. Endocrinology. 2000; 141:4801–4804. [PubMed: 11108297]

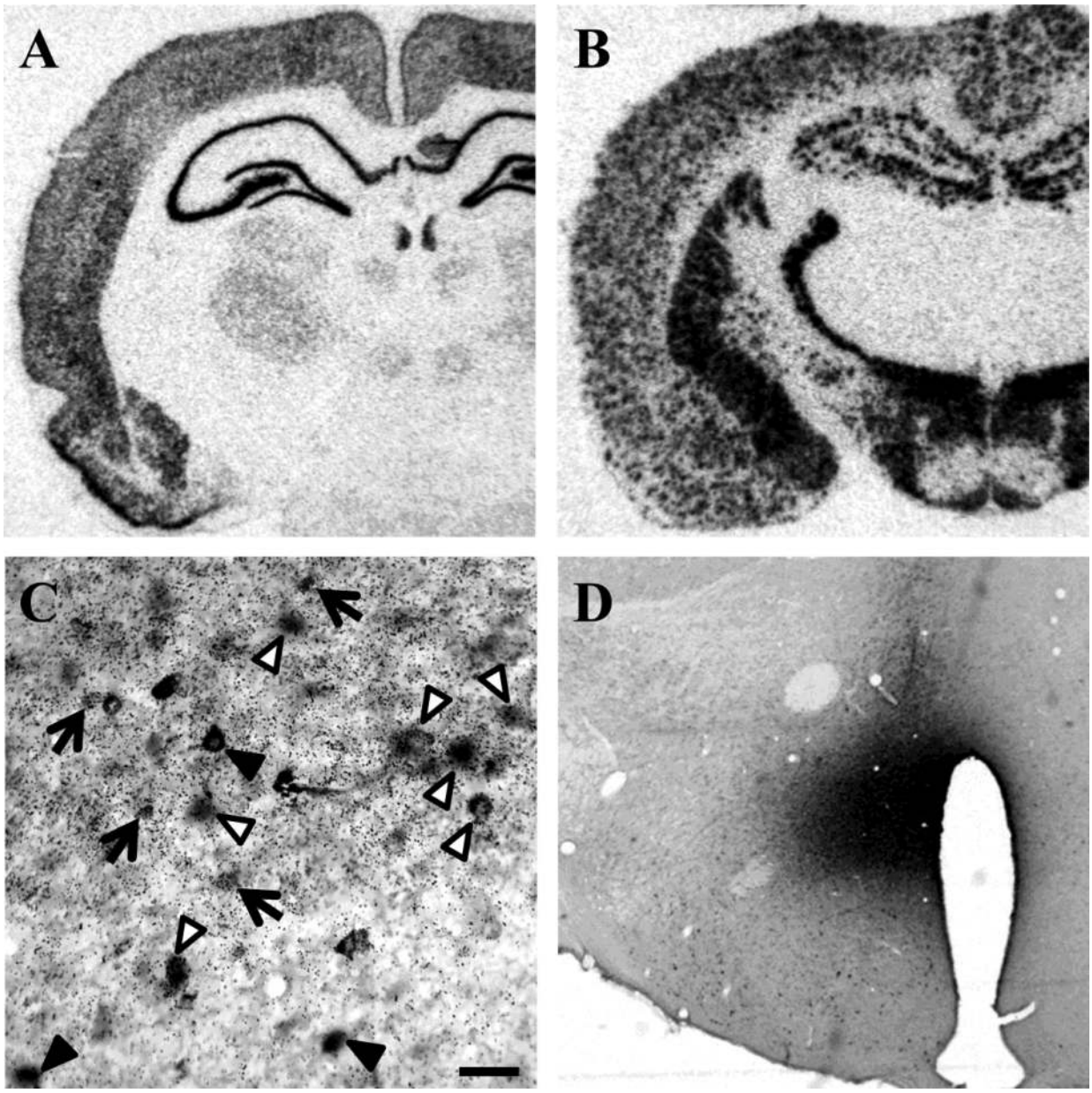

Figure 1.

Hybridization of vGluT1 mRNA (**A**) and GAD65 mRNA (**B**) demonstrate robust and selective signals for glutamatergic and GABAergic markers, respectively. (**C**) Criteria for determining co-localization of FG and GAD65 mRNA at the ventrolateral boundary of the DMH: white arrow heads indicate cells that are FG+/GAD65+, black arrow heads point to FG positive cells that do not co-localize with GAD65 mRNA, and black arrows designate cellular aggregations of GAD65 mRNA in the absence of FG immunoreactivity. A representative FG injection site in the DMH is depicted in panel **D**. Scale bar = 50 μm.

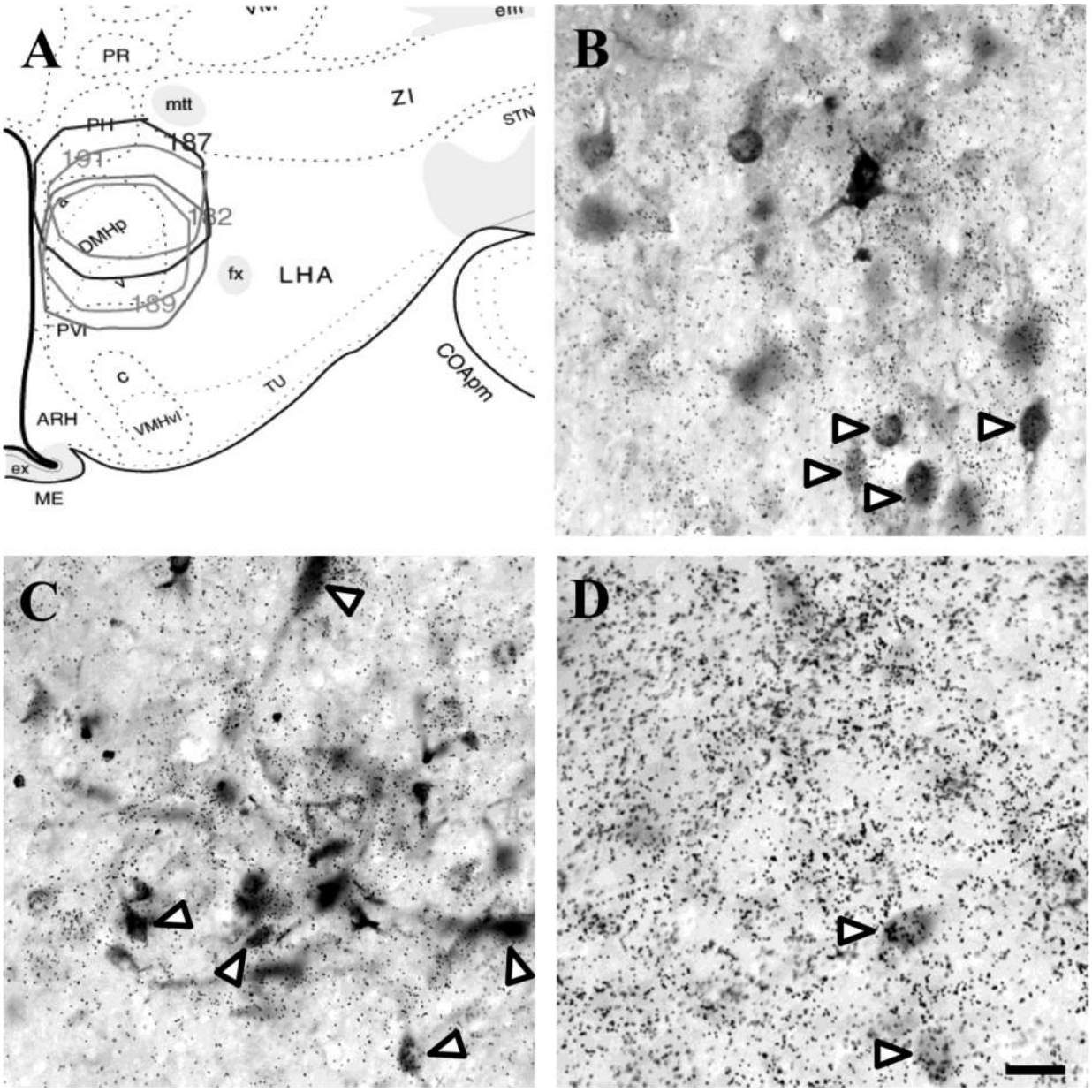

Figure 2.

Distribution of injections into the DMH demonstrates the spread of FG (**A**). Significant co-localization of FG and vGluT2 in the dorsal aspect of the PVT (**B**) signifies an excitatory input to the DMH. Inhibitory input to the DMH is indicated by GAD65 and FG co-localization in the fusiform portion of the BST (**C**) and medial division of the CeA (**D**). White arrow heads indicate co-localization. Scale bar = 50 μm.

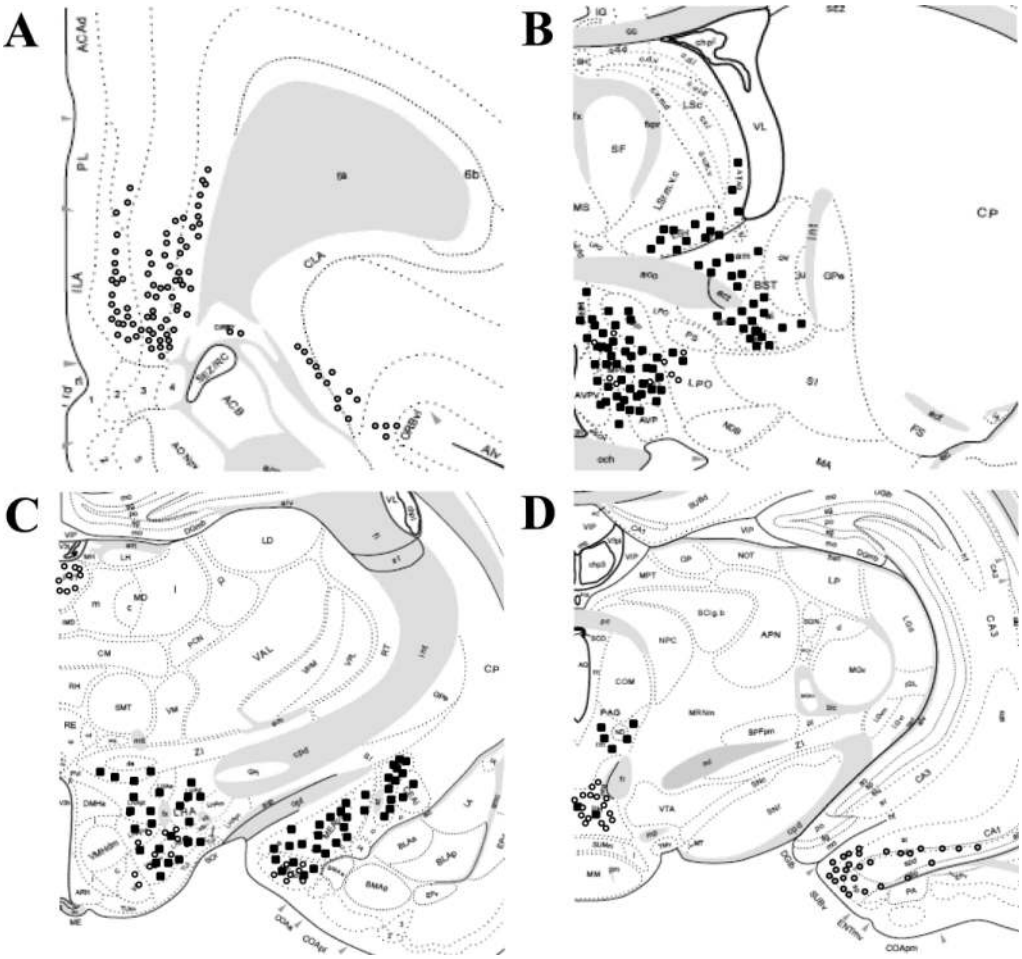

Figure 3.

Limbic glutamatergic and GABAergic input to the DMH. Major sites of FG co-localization with vGluT1 (grey circles), vGluT2 (white circles), and GAD65 (black squares) are indicated in schematic adaptations from the atlas of Swanson (2004). Distances from bregma: +2.8 mm (**A**), -0.26 mm (**B**), -2.45 mm (**C**), and -5.00 mm (**D**).

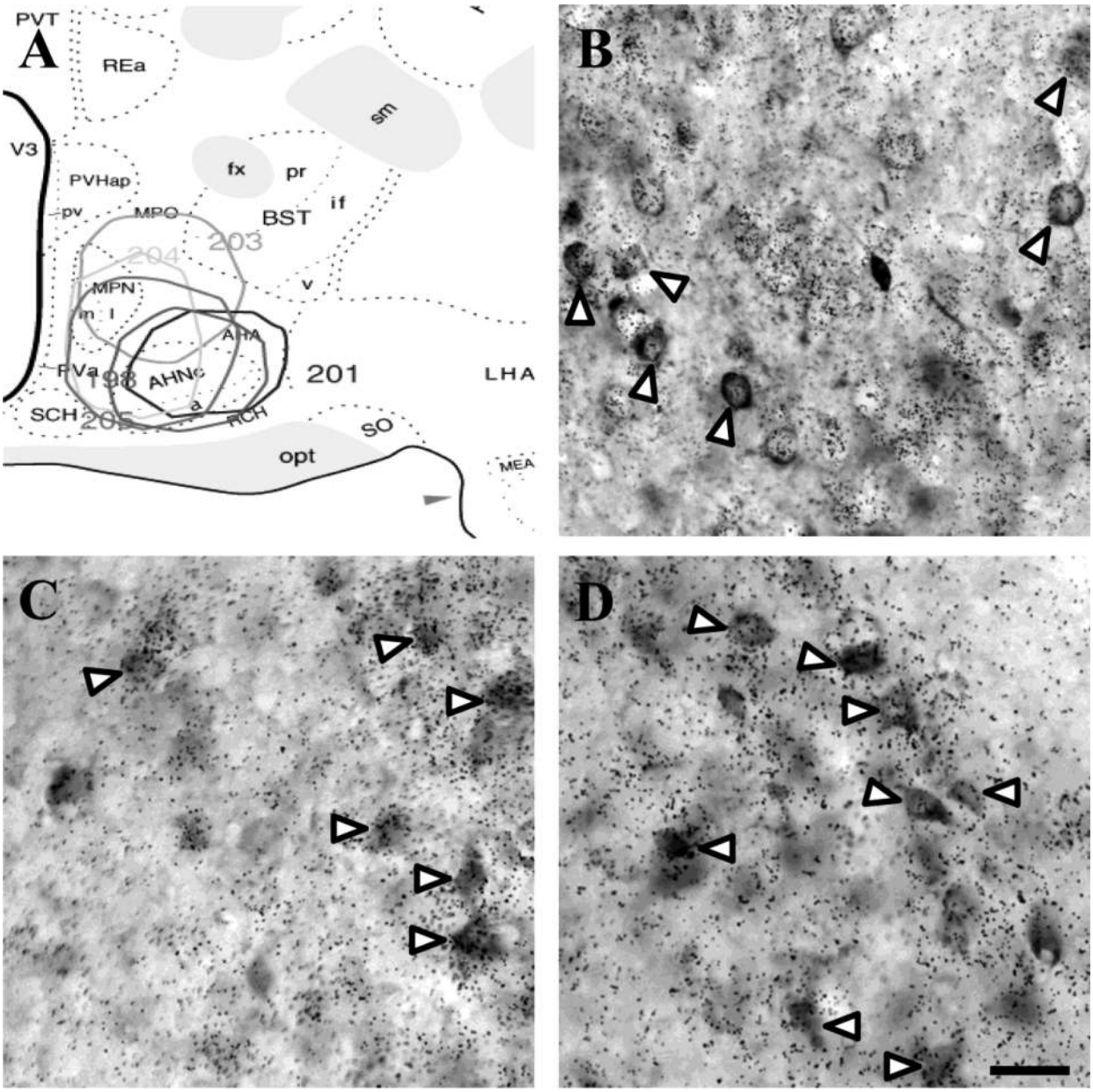

Figure 4.

Distribution of injections into the mPOA encompassing the AHN and MPN (**A**). The mPOA received predominantly GABAergic (GAD65+) input from the ventral LS (**B**), anteromedial BST (**C**), and posterodorsal MeA (**D**). White arrow heads indicate co-localization. Scale bar = 50 μm.

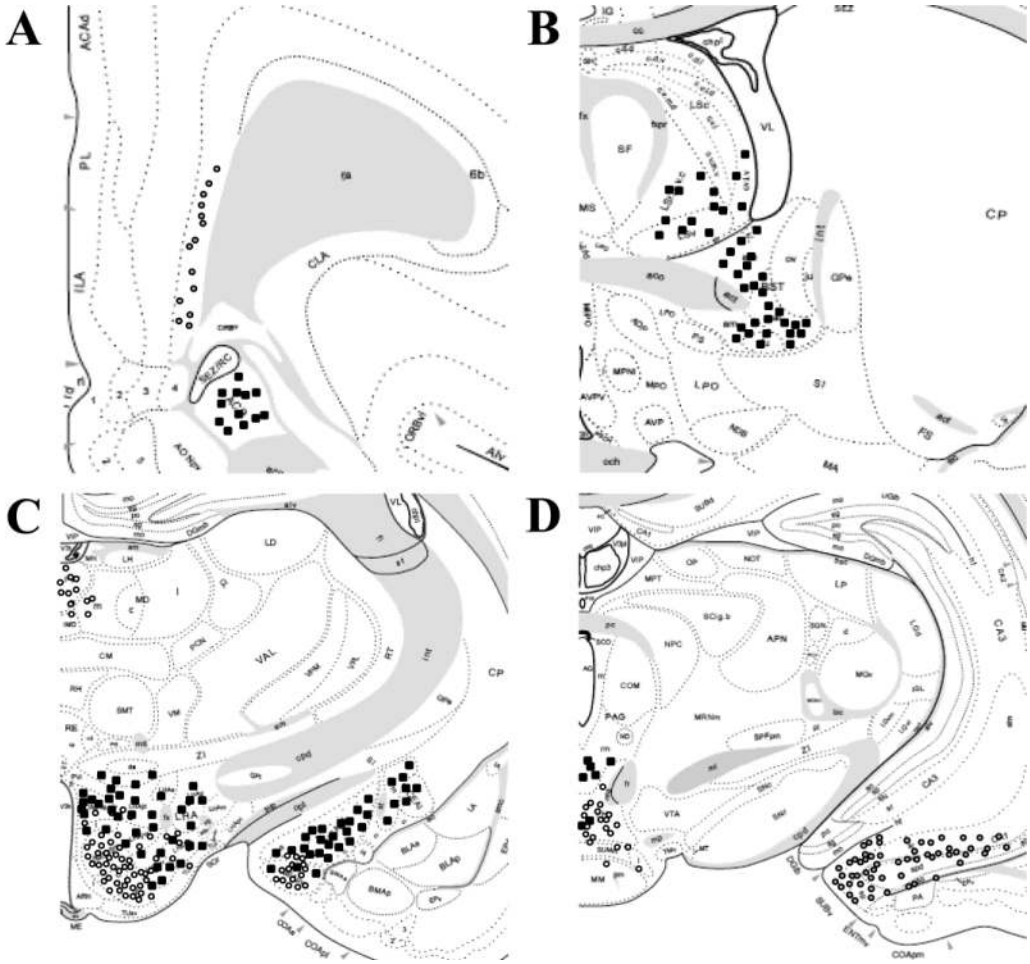

Figure 5.

Limbic glutamatergic and GABAergic input to the mPOA. Major sites of FG co-localization with vGluT1 (grey circles), vGluT2 (white circles), and GAD65 (black squares) are indicated in schematic adaptations from the atlas of Swanson (2004). Distances from bregma: +2.8 mm (**A**), -0.26 mm (**B**), -2.45 mm (**C**), and -5.00 mm (**D**).

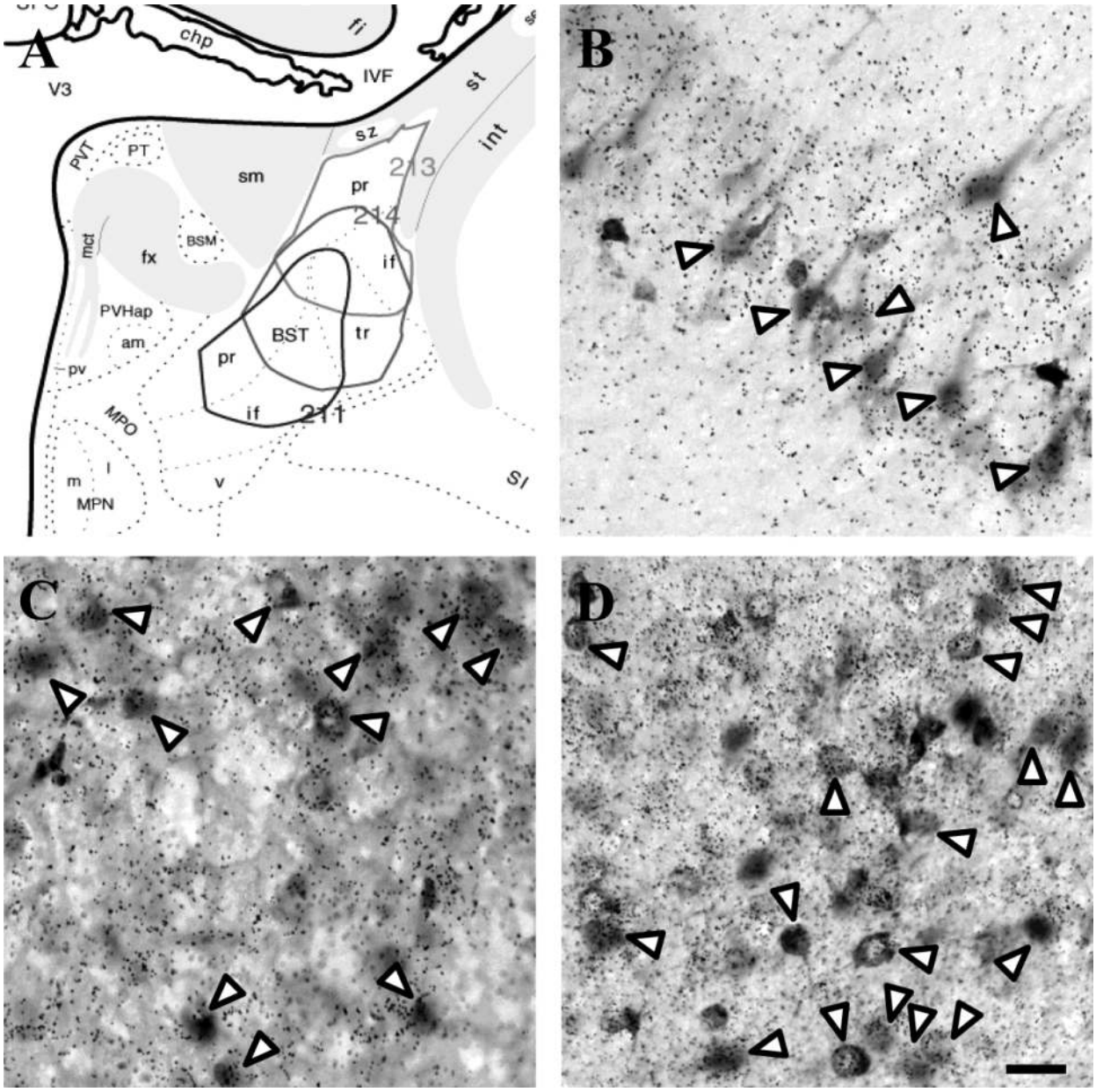

Figure 6.

Injection sites targeting the posterior subnuclei of the BST (**A**). Excitatory input to the BST arose from the vGluT1-positive vSub (**B**) and vGluT2-positive anterior PVT (**C**). A large number of FG-labeled cells were present in the medial CeA, most of which co-localized with GAD65 mRNA (**D**). White arrow heads indicate co-localization. Scale bar = 50 μm.

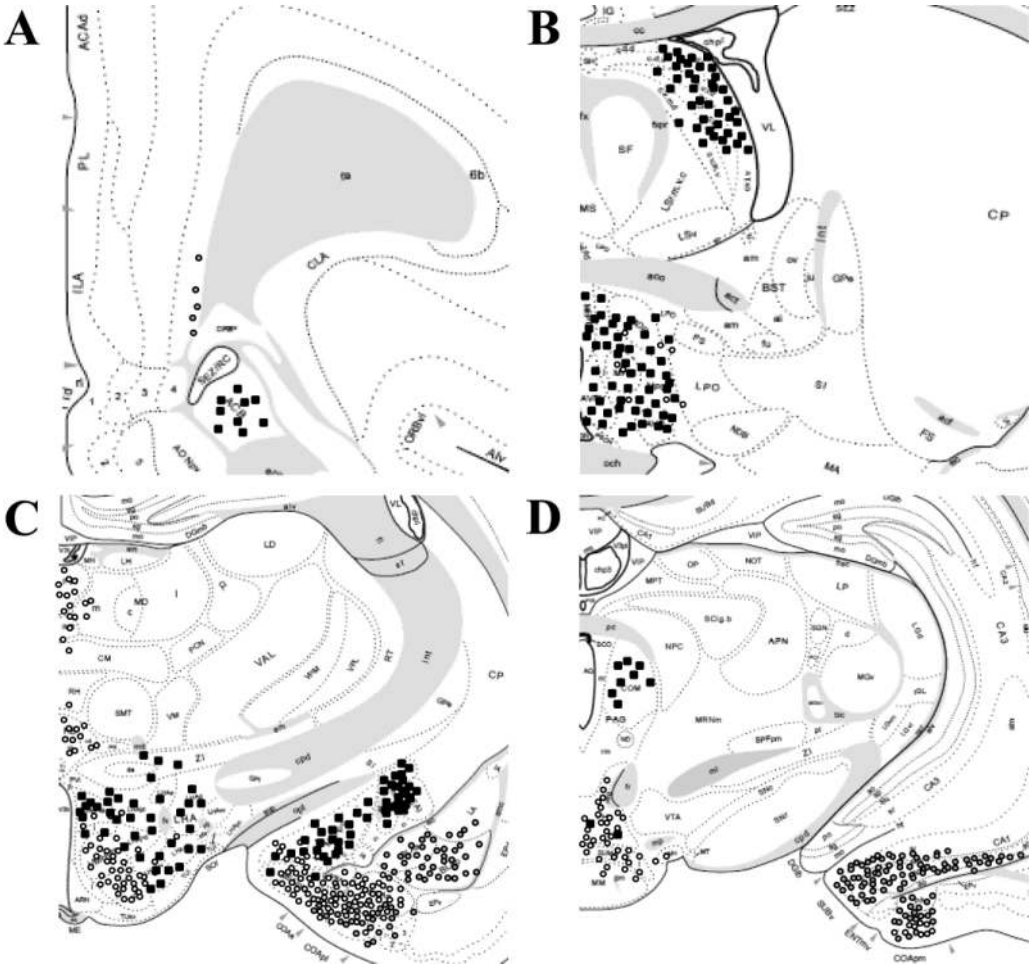

Figure 7.

Limbic glutamatergic and GABAergic input to the posterior BST. Major sites of FG co-localization with vGluT1 (grey circles), vGluT2 (white circles), and GAD65 (black squares) are indicated in schematic adaptations from the atlas of Swanson (2004). Distances from bregma: +2.8 mm (**A**), -0.26 mm (**B**), -2.45 mm (**C**), and -5.00 mm (**D**).

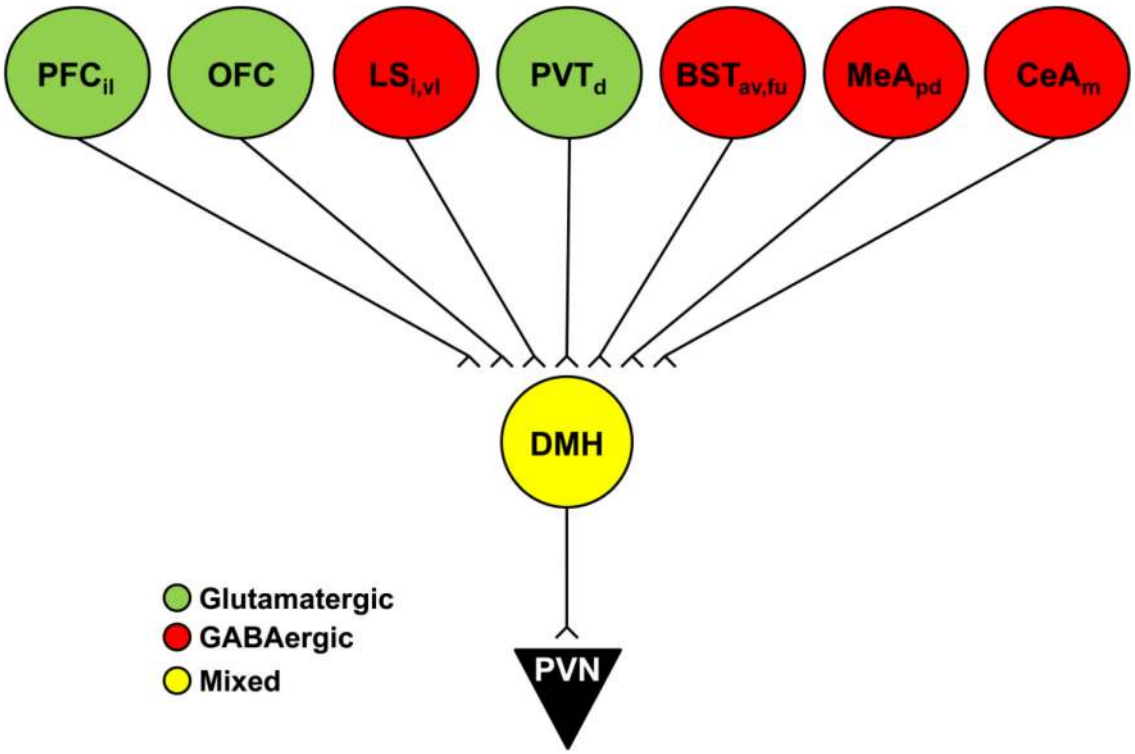

Figure 8.

Schematic illustration summarizing the phenotype of prominent limbic inputs to the DMH. Green indicates glutamatergic input, red GABAergic input, and yellow mixed glutamate and GABA. av: anteroventral, d: dorsal, i: intermediate, il: infralimbic, fu: fusiform, m: medial, pd: posterodorsal, vl: ventrolateral.

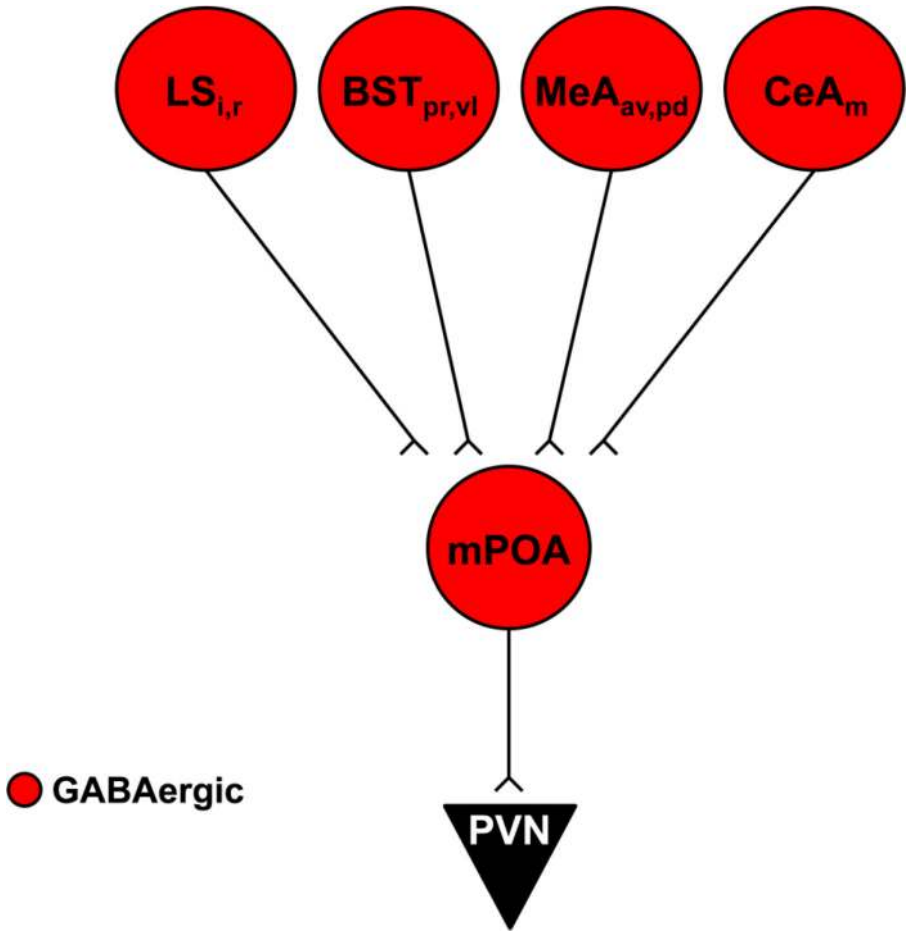

Figure 9.

Schematic illustration summarizing the phenotype of prominent limbic inputs to the mPOA. Green indicates glutamatergic input, red GABAergic input, and yellow mixed glutamate and GABA. av: anteroventral, i: intermediate, m: medial, pd: posterodorsal, pr: principal, r: rostal, vl: ventrolateral.

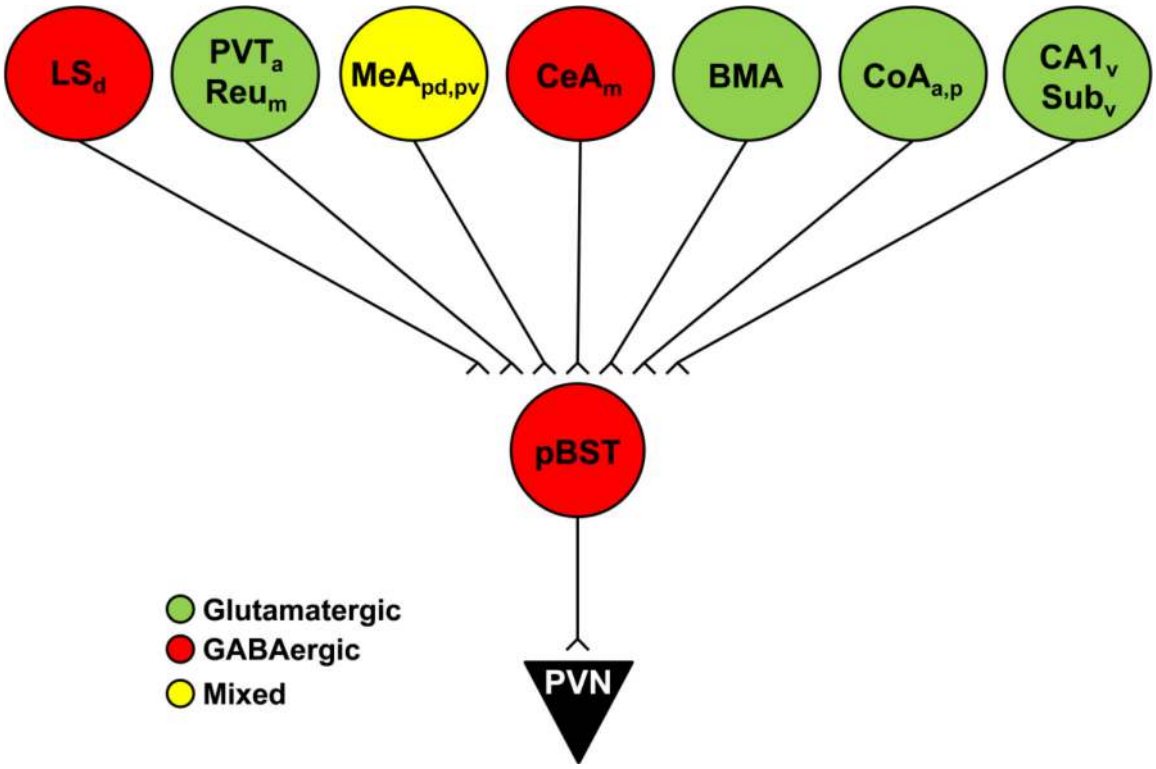

Figure 10.

Schematic illustration summarizing the phenotype of prominent limbic inputs to the pBST. Green indicates glutamatergic input, red GABAergic input, and yellow mixed glutamate and GABA. a: anterior, d: dorsal, m: medial, p: posterior, pd: posterodorsal, pv: posteroventral, Reu: reunions, v: ventral.

Table 1

Phenotypic analysis of the major limbic inputs to the dorsomedial hypothalamus

	GAD65+/FG+	vGluT1+/FG+	vGluT2+/FG+
Cortex			
infralimbic	-	++	-
orbitofrontal	-	++	-
prelimbic	-	++	-
Lateral Septum			
intermediate	+++	-	-
ventrolateral	+++	-	-
Amygdala			
central, lateral	++	-	-
central, medial	+++	-	-
medial, pd	+++	-	-
medial, pv	++	-	-
Bed Nucleus of the Stria Terminalis			
anterodorsal	++	-	-
anterolateral	++	-	-
anteromedial	++	-	-
anteroventral	+++	-	-
fusiform	+++	-	-
interfascicular	++	-	-
principal	++	-	-
transverse	++	-	-
ventral	++	-	-
Hypothalamus			
anterior	++	-	-
lateral	+	-	-
medial preoptic	++	-	-
posterior	+	-	++
Periaqueductal gray			
dorsolateral	++	-	-
rostral	+	-	-
Other			
subiculum, v	-	++	-
thalamus, pvt	-	-	++

(-) widely scattered dual-labeled cells (substantially less than 25% of cells); (+) dual-labeling in 25-50% of cells; (++) dual-labeling in the majority of cells (50-75%); (+++) most, if not all, FG+ cells double-labeled. n =4. pd: posterodorsal, pv: posteroventral, pvt: paraventricular, v: ventral

Table 2

Phenotypic analysis of the major limbic inputs to the medial preoptic area

	GAD65+/FG+	vGluT1+/FG+	vGluT2+/FG+
Nucleus Accumbens			
core	+	-	-
shell	++	-	-
Lateral Septum			
intermediate	+++	-	-
rostral	+++	-	-
ventrolateral	+++	-	-
Amygdala			
central, medial	+++	-	-
medial, ad	+++	-	-
medial, av	+++	-	-
medial, pd	++	-	-
medial, pv	+	-	++
Hippocampus			
CA1, ventral	-	++	-
subiculum, v	-	++	-
Bed Nucleus of the Stria Terminalis			
anterodorsal	++	-	-
anterolateral	+++	-	-
anteromedial	++	-	-
fusiform	++	-	-
interfascicular	++	-	-
principal	+++	-	-
transverse	++	-	-
ventrolateral	+++	-	-
Hypothalamus			
dorsomedial, d	++	-	+
dorsomedial, v	++	-	-
lateral	++	-	+
perifornical	++	-	-
posterior	+	-	++
ventromedial	-	-	+++
Periaqueductal gray			
medial	+	-	-
rostromedial	+	-	-
ventrolateral	+	-	-
Other			
thalamus, pvt	-	-	++

(-) widely scattered dual-labeled cells (substantially less than 25% of cells); (+) dual-labeling in 25-50% of cells; (++) dual-labeling in the majority of cells (50-75%); (+++) most, if not all, FG+ cells double-labeled. n = 5. ad: anterodorsal, av: anteroventral, d: dorsal, p: posterior, pd: posterodorsal, pv: posteroventral, pvt: paraventricular, v: ventral

Table 3

Phenotypic analysis of the major limbic inputs to the posterior bed nucleus of the stria terminalis

	GAD65+/FG+	vGluT1+/FG+	vGluT2+/FG+
Nucleus Accumbens			
core	+	-	-
shell	++	-	-
Lateral Septum			
caudal	+++	-	-
dorsolateral	+++	-	-
Amygdala			
basolateral	-	++	-
basomedial	-	+	++
central, lateral	+++	-	-
central, medial	+++	-	-
cortical, a	-	+	++
cortical, p	-	++	+
medial, ad	+++	-	-
medial, pd	++	-	-
medial, pv	-	-	++
posterior	-	++	-
Hippocampus			
CA1, ventral	-	+++	-
subiculum, v	-	+++	-
Thalamus			
paraventricular	-	-	++
reunions	-	-	++
Hypothalamus			
anterior	++	-	+
dorsomedial, d	++	-	+
dorsomedial, v	++	-	-
lateral	++	-	+
perifornical	++	-	-
posterior	-	-	++
preoptic	++	-	-
ventromedial	-	-	+++
Mammilary			
medial	-	-	++
supra	-	-	++
tubero	-	-	++

(-) widely scattered dual-labeled cells (substantially less than 25% of cells); (+) dual-labeling in 25-50% of cells; (++) dual-labeling in the majority of cells (50-75%); (+++) most, if not all, FG+ cells double-labeled. n = 3. a: anterior, ad: anterodorsal, d: dorsal, p: posterior, pd: posterodorsal, pv: posteroventral, v: ventral